International J. of Pure & Engg. Mathematics (IJPEM)
ISSN 2348-3881, Vol. 4 No. III (December, 2016), pp. 31-42

# FRACTURE STRENGTH DETERMINATION OF MARAGING STEEL ROCKET MOTOR CASES - A COMPARATIVE STUDY OF ANALYTICAL AND EXPERIMENTAL DATA

**S. SUNDARESAN[1], SREEDEVI LEKSHMI[2] AND B. NAGESWARA RAO[3]**

[1] Scientist, Structural Design and Analysis Division,
Vikram Sarabhai Space Centre, Trivandrum, India
[2] Lecturer, Department of Civil Engineering,
Sree Buddha College of Engineering, Pattoor, Kerala, India
[3] Professor, Department of Mechanical Engineering,
School of Mechanical and Civil Sciences, University, Vaddeswaran, India

**Abstract**

Maraging steels are greatly employed for the fabrication of rocket motor cases because of its high strength and fracture toughness. They are low carbon, high nickel, iron base alloys. Maraging steels can be easily machined, formed and welded. Defects like cracks or flaws are developed in this material during fabrication process. Cracks generally have sharp edges and therefore sensitive for initiation of crack growth and fracture. This paper deals with a procedure to determine the fracture strength of structural component in the presence of crack. Fracture strength plays a vital role in determining critical stress intensity factor for any structural component. Equation for the determination of fracture strength of maraging steel is presented. The relationship between failure strength and critical stress intensity factor is briefly discussed. A limited number of surface cracked tension specimens made of maraging steel material having different width and crack sizes are used to derive fracture strength. The analytical results of fracture strength are determined

---

Key Words : *Maraging steel, Fracture strength, Crack size, Motor cases, Critical stress intensity factor, Surface cracked tension specimen, Failure assessment diagram.*

using fracture parameters of maraging steel. Fracture strength obtained from test data are compared with analytical results and the relative error is presented. Failure assessment diagram in terms of critical stress intensity factor and failure stress is presented. Results are discussed.

## 1. Introduction

Maraging steel is currently being used for construction of space vehicle pressure vessels. It possesses superior properties like high strength and toughness due to a combination of two solid state reactions, "MAR + AGING", meaning martensitic transformation and subsequent ageing. It has the composition of 18% Ni, 8% Co and 5% Mo as a primary alloying element. Resistance of such high strength materials is sensitive to the presence of crack like defects. The specified mechanical properties are:

Plane strain fracture toughness, $K_{IC} \geq 90MPa\sqrt{m}$

Yield strength, $\sigma_{ys} \geq 1725MPa$

Ultimate tensile strength, $\sigma_{ult} \geq 1765MPa$

Weld efficiency $\geq 90\%$.

The significant parameters to specify the critical crack size in structure are the applied load levels, the fracture toughness, the location of crack and its orientation. The theoretical determination of failure load and especially the failure process of flawed structural components are indispensable in the performance of safety analysis. In addition to the generally very complex and expensive finite element methods, approximate analytical methods have been developed to assess the load bearing capacity of flawed structural components with a relatively low cost and computational time [1].

## 2. Fracture Strength of Center Cracked Tensile Specimens

Several structural analysis methods to predict the fracture behavior of cracked structural components were explained in detail by various researchers. Several fracture analysis methods to predict the fracture behavior of flawed structural components used in an experimental and predictive round robin conducted in 1970-'80 by American Society for Testing Materials (ASTM) Task Group E 24.06.02 are : Linear - elastic fracture mechanics (LEFM) corrected for size effects or plastic yielding; Equivalent energy; The Two-parameter fracture criterion (TPFC); The deformation plasticity failure assessment diagram (DPFAD); The theory of ductile fracture; [2] The $K_R$.curve with the Dugdale model; An effective $K_R$ - curve derived from residual strength data; The effective KR-curve with a limit load condition; Limit-load analyses; A twodimensional finite element analysis using a critical crack - tip opening displacement criterion with stable crack growth; A three-dimensional finite element analysis using a critical crack- front singularity parameter with a stationary crack. In this paper, equation for fracture strength for a finite width tension plate containing central surface crack is presented.

The stress intensity factor ($K_I$) for a finite width plate containing a center surface crack of length **2c** and depth **a** as shown in fig. 1 is

$$K_I = (\sigma M (\pi a)^{0.5})/\phi. \tag{1}$$

Here, $\sigma$ is the applied stress, $\phi$ is the flaw shape parameter, $M$ is the magnification factor, $W$ is the width of the plate and '$t$' is the thickness of the plate. [3]

The magnification factor ($M$), finite width correction factor ($f_w$), flaw shape parameter ($\phi$) in terms of the crack depth ($a$), half the crack length ($c$), width ($W$) and thickness ($t$) are:

$$M = M_e f_w; \quad M_e = M_1 + \left(\phi\sqrt{\frac{c}{a}} - M_1\right) \times \left(\frac{a}{t}\right)^q; \tag{2}$$

$$\begin{aligned}
M_1 &= 1.13 - 0.1 \times \left(\frac{a}{c}\right) \quad \text{for} \quad a \leq c; \\
M_1 &= \left(1 + 0.03\left(\frac{a}{c}\right)\right)\sqrt{\frac{c}{a}} \quad \text{for} \quad a \geq c; \\
\phi^2 &= 1 + 1.464\left(\frac{a}{c}\right)^{1/65} \quad \text{for } a \leq c; \\
\phi^2 &= 1 + 1.464\left(\frac{c}{a}\right)^{1.65} \quad \text{for} \quad a \geq c; \\
f_w &= \sqrt{sec\left(\frac{\pi c}{W}\sqrt{\frac{a}{t}}\right)}; \quad q = 2 + 8x\left(\frac{a}{c}\right)^3.
\end{aligned}$$

When the depth '$a$' of the crack is equal to the thickness ($t$), equation (6.11) gives the stress intensity factor for finite width tension specimens having a centre through-crack. Equation (1.0) holds good for both through and surface crack tension specimens.

Equating the fracture toughness ($K_{IC}$) of the material to the stress intensity factor ($K_I$), one can find the fracture strength ($\sigma_f$) of a finite width plate containing a surface crack. Fracture strength ($\sigma_f$) equation is given as follows:

$$\begin{aligned} \sigma_j &= \sigma_{ult}\left[1-\left(\frac{2}{3\sqrt{3}}\frac{\sigma_{ult}}{K_{IC}}\frac{M\sqrt{\pi a}}{\phi}\right)^2\right] \quad \text{for} \quad \sigma_f \geq \tfrac{2}{3}\sigma_{ult} \\ &= \frac{K_{IC}\phi}{M\sqrt{\pi a}} \quad \text{for} \quad \sigma_f \leq \tfrac{2}{3}\sigma_{ult} \end{aligned} \tag{3}$$

$$\begin{aligned} \sigma_f &= \sigma_{ult}\left[1-\left(\frac{2}{3\sqrt{3}}\frac{\sigma_{ult}}{K_{IC}}\frac{M\sqrt{\pi a}}{\phi}\right)^2\right] \quad \text{for} \quad \sigma_f \geq \tfrac{2}{3}\sigma_{ult} \\ &= \frac{K_{IC}\phi}{M\sqrt{\pi a}} \quad \text{for} \quad \sigma_f \leq \tfrac{2}{3}\sigma_{ult} \end{aligned} \tag{4}$$

From this expression fracture strength of M250 and M300 maraging steel rocket motor case surface cracked tension specimens are evaluated. The results are compared with available test data and presented in the Tables. Based on the three parameter relationship among critical stress intensity factor ($K_{\max}$), the fracture strength ($\sigma_f$) and the ultimate strength ($\sigma_{ult}$), failure analysis diagram is presented and one can easily understand the range of $K_{\max}$ over $\sigma_f$ and $\sigma_{ult}$. In addition to the determination of fracture strength, an attempt is made to determine the failure load of 30 CT specimens and the results are compared with the test data. Equation for failure load is as follows: where $W$ is the width, $B$ the thickness and $a_0$ is the initial crack length of specimen; $\sigma_{ult}$, the ultimate strength and $P_{\max}$ is the failure load of the specimen tested. Failure load expression [2] is given as follows:

$$P_{\max} = 0.815BW\sigma_{ult}(1-a_0/W)^2(2+a_0/W)^{-1}\{0.3927+0.0402(a_0/W)+0.6268(a_0/W)^2\}. \tag{6}$$

**Table 1: Failure load $P_{\max}$ of the M250 grade maraging steel CT specimens**

| $\sigma_{ult}$ (MPa) | W(mm) | B(mm) | $a_0$ (mm) | $P_{max}$ (test) ($kN$) | $P_{max}$ (eqn.2) ($kN$) |
|---|---|---|---|---|---|
| 1859 | 14.98 | 7.62 | 7.720 | 9.48 | 9.31 |
| 1761 | 15.00 | 7.62 | 7.377 | 9.28 | 9.55 |
| 1760 | 15.02 | 7.62 | 7.440 | 9.04 | 9.45 |
| 1798 | 14.98 | 7.62 | 7.486 | 9.09 | 9.49 |
| 1791 | 15.01 | 7.62 | 7.520 | 9.19 | 9.43 |
| 1843 | 15.64 | 7.80 | 8.570 | 9.21 | 8.76 |

| $\sigma_{ult}$ (MPa) | W(mm) | B(mm) | $a_0$ (mm) | $P_{max}$ (test) ($kN$) | $P_{max}$ (eqn.2) ($kN$) |
|---|---|---|---|---|---|
| 1782 | 15.59 | 7.80 | 7.788 | 10.4 | 10.0 |
| 1782 | 15.62 | 7.80 | 7.833 | 10.3 | 9.98 |
| 1821 | 15.54 | 7.80 | 7.747 | 10.7 | 10.3 |
| 1790 | 15.56 | 7.79 | 7.147 | 11.5 | 11.4 |
| 1766 | 15.61 | 7.80 | 7.903 | 9.65 | 9.73 |
| 1781 | 15.55 | 7.80 | 7.660 | 11.0 | 10.2 |
| 1781 | 15.54 | 7.80 | 7.742 | 10.0 | 10.0 |
| 1815 | 15.62 | 7.80 | 7.740 | 10.7 | 10.4 |
| 1793 | 15.60 | 7.79 | 7.917 | 10.3 | 9.82 |
| 1846 | 15.63 | 7.81 | 8.080 | 10.4 | 9.83 |
| 1763 | 15.57 | 7.83 | 8.045 | 10.0 | 9.38 |
| 1790 | 15.57 | 7.80 | 8.152 | 9.90 | 9.30 |
| 1796 | 15.61 | 7.79 | 7.890 | 11.0 | 9.91 |
| 1817 | 15.59 | 7.80 | 7.223 | 11.4 | 11.5 |
| 1829 | 15.61 | 7.80 | 7.892 | 10.5 | 10.1 |
| 1829 | 15.60 | 7.80 | 8.175 | 9.82 | 9.47 |
| 1780 | 15.58 | 7.80 | 7.620 | 10.9 | 10.4 |
| 1821 | 15.67 | 7.81 | 7.703 | 9.88 | 10.6 |
| 1878 | 15.63 | 7.80 | 7.741 | 10.3 | 10.8 |
| 1847 | 15.64 | 7.79 | 7.713 | 10.9 | 10.6 |
| 1842 | 15.64 | 7.79 | 7.333 | 11.9 | 11.5 |
| 1872 | 15.56 | 7.78 | 7.170 | 11.2 | 11.9 |
| 1822 | 15.54 | 7.82 | 8.123 | 9.90 | 9.46 |
| 1814 | 15.59 | 7.82 | 7.868 | 9.90 | 10.1 |

## 3. Importance of $K_{\max}$ and $\sigma_f$ Relationship

Understanding the failure of materials plays an important role in the design and manufacturing process. When dealing with a specific material for a particular application, it is not clearly established whether plain strain fracture toughness ($K_{IC}$) should be used or plane stress condition. The $K_{IC}$ seems to be important in heavy sections like forging or thick plate. This is the reason why plane strain fracture toughness is used in thick sectional structural member in aerospace applications. [4]

ASTM-E561 suggests generation of an R-curve from through the test coupons of CT specimens. It should be noted $K_{IC}$ is geometry dependent where as R-curve is considered to be a material property independent of geometry. Therefore R-curve of material will be useful for the accurate determination of critical load of the through cracked specimen. For part through cracked configurations, fracture strength estimations are not possible directly from the R-curve of the material because the part through crack has two dimensions, namely crack length and its depth. In such situations, development of a relationship between the failure stress and the stress intensity factor at failure will be useful for fracture strength evaluation of cracked configurations.

Rao et al derived a relation between the stress intensity factor and corresponding stress at failure for cracked configurations using crack-growth resistance curve (R-curve) of the material from CT specimens. The failure stress decreases with the increase of crack size. When the crack size is negligibly small, failure stress tends to the ultimate strength of the material. Since the stress intensity factor ($K_I$) is a function of load, geometry and crack size, it is more appropriate to have a relationship between stress intensity factor at failure $K_{\max}$ and the failure stress from the fracture data of cracked specimens and this is useful for fracture strength evaluation of flawed configuration. [5]

The relationship between $K_{\max}$ and $\sigma_f$ can be of the form

$$K_{\max} = K_F\{1 - m(\sigma_f/\sigma_{ult}) - (1-m)(\sigma_f/\sigma_{ult})^p\} \tag{5}$$

where, $\sigma_f$ is the failure stress normal to the direction of the crack in a body and $\sigma_{ult}$ is the normal stress required to produce a plastic hinge on the net section. For centre crack tension specimen, failure stress is equal to ultimate stress of the material. For the pressurized cylinders, failure stress is the hoop stress at the failure pressure of the flawed cylinder and ultimate stress is the hoop stress at failure pressure of an unflawed cylinder. In the above equation, $K_F$, $m$ and $p$ are fracture parameters derived from fracture test data. The above equation is known as three parameter fracture criterion which was derived from the conventional two parameter criteria. It is a well known fact that the tensile strength of a specimen decreases with increasing crack size. If the failure stress is less than the yield stress, then there exists a linear relationship between $\sigma_f$ and $K_{\max}$. For small sizes of cracks where $\sigma_{ys} < \sigma_f < \sigma_u$, the relationship between between $\sigma_f$ and $K_{\max}$ is expected to be non linear. $\sigma_{ys}$ is the 0.2% proof stress or yield stress of the material.

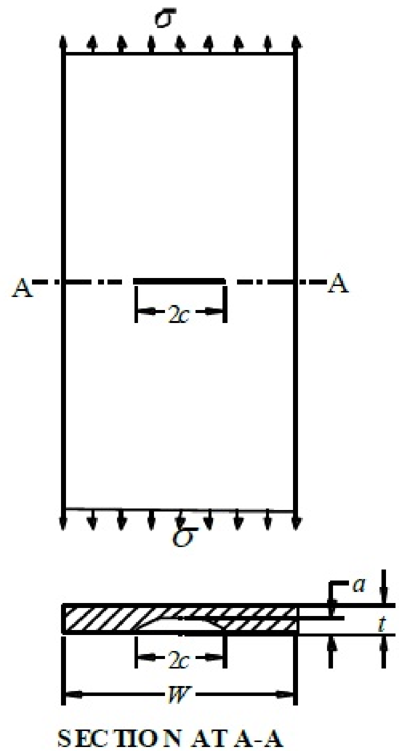


Fig 1: Finite width tension plate containing a center surface crack

In the following Tables given, SCT specimens data of M250 and M300 grade maraging steel are considered for comparison of fracture strength of analytical and experimental data, wherein $w$ is the width of the specimen, **2c** × **a** is the size of the crack ('$2c$', length and '$a$' being the depth of a surface crack) and $K_F$, $m$ and $p$ are fracture parameters.

**Table 2 : Comparison of analytical and experimental fracture strength of M300 grade maraging steel SCT specimens[6]**

$(t = 3mm, \sigma_{ult} = 2255MPa, K_F = 151.7MPa\sqrt{m}, m = 0.4, p = 15.8)$

| Width(mm) | Crack Dimensions (mm) | | Fracture strength $\sigma_f(MPa)$ | | |
|---|---|---|---|---|---|
| $w$ | $a$ | $2c$ | Test | Analysis | Relative Error (%) |
| 15.2 | 0.8 | 4.0 | 2008.0 | 1879.8 | 6.4 |
| 15.2 | 1.1 | 5.0 | 1668.5 | 1705.7 | -2.2 |
| 15.1 | 1.1 | 5.8 | 1566.8 | 1646.4 | -5.1 |
| 19.6 | 1.4 | 7.5 | 1426.9 | 1446.8 | -1.4 |

| Width(mm) | Crack Dimensions (mm) | | Fracture strength $\sigma_f(MPa)$ | | |
|---|---|---|---|---|---|
| $w$ | $a$ | $2c$ | Test | Analysis | Relative Error (%) |
| 18.4 | 1.4 | 7.2 | 1367.9 | 1458.8 | -6.7 |
| 19.1 | 1.7 | 9.0 | 1349.1 | 1259.7 | 6.6 |
| 18.5 | 1.7 | 7.5 | 1220.0 | 1349.1 | -10.6 |

Standard error obtained is 0.063.

**Table 3 : Comparison of analytical and experimental fracture strength of M300 grade maraging steel cylindrical vessels having surface cracks [6].**

$(D_0 = 77.2mm, t = 3mm, \sigma_{ys} = 2120MPa, \sigma_{ult} = 2255MPa, K_F = 148.6MPa\sqrt{m}, m = 0.4, p = 15.8)$

| Crack Dimensions (mm) | | Fracture strength $\sigma_f(MPa)$ | | |
|---|---|---|---|---|
| $a$ | $2c$ | Test | Analysis | Relative Error (%) |
| 0.4 | 2.5 | 193.8 | 174.6 | 9.9 |
| 0.9 | 4.0 | 157.7 | 157.2 | 0.3 |
| 1.0 | 5.5 | 158.6 | 145.9 | 8.0 |
| 1.4 | 5.2 | 144.0 | 139.8 | 3.0 |
| 1.6 | 10.0 | 105.7 | 105.5 | 0.2 |
| 1.7 | 12.0 | 99.0 | 96.6 | 2.5 |
| 1.7 | 8.0 | 117.7 | 112.7 | 4.3 |
| 1.8 | 14.0 | 94.3 | 85.3 | 9.5 |

Standard error obtained is 0.06.

**Table 4: Comparison of analytical and experimental fracture strength of M250 grade maraging steel parent metal SCT specimens [7]**

$(W = 15mm, t = 7.5mm, \sigma_{ult} = 1860MPa, K_F == 235.7MPa, m = 0.6, p = 20.4)$

| Crack Dimensions (mm) | | Fracture strength $\sigma_f(MPa)$ | | |
|---|---|---|---|---|
| $a$ | $2c$ | Test | Analysis | Relative Error (%) |
| 1.3 | 2.7 | 1850 | 1746.4 | 5.6 |
| 1.4 | 3.0 | 1850 | 1737.0 | 6.1 |
| 1.5 | 3.4 | 1840 | 1719.3 | 6.6 |
| 1.7 | 3.8 | 1831 | 1702.1 | 7.0 |

| Crack Dimensions (mm) | | Fracture strength $\sigma_f(MPa)$ | | |
|---|---|---|---|---|
| $a$ | $2c$ | Test | Analysis | Relative Error (%) |
| 1.7 | 4.1 | 1820 | 1689.5 | 7.2 |
| 1.7 | 4.3 | 1830 | 1681.3 | 8.1 |
| 1.8 | 4.0 | 1822 | 1692.9 | 7.1 |
| 2.0 | 4.0 | 1830 | 1691.9 | 7.5 |
| 1.9 | 4.8 | 1798 | 1656.1 | 7.9 |
| 2.0 | 4.9 | 1800 | 1651.8 | 8.2 |
| 2.0 | 4.5 | 1786 | 1668.3 | 6.6 |
| 2.0 | 4.4 | 1802 | 1673.0 | 7.2 |
| 2.2 | 4.8 | 1783 | 1651.1 | 7.4 |
| 2.0 | 5.0 | 1788 | 1644.8 | 8.0 |
| 2.2 | 5.3 | 1771 | 1625.5 | 8.2 |
| 2.2 | 5.7 | 1760 | 1605.2 | 8.8 |
| 2.3 | 5.9 | 1760 | 1591.5 | 9.6 |
| 2.5 | 5.8 | 1754 | 1590.7 | 9.3 |
| 2.5 | 6.3 | 1711 | 1562.5 | 8.7 |
| 2.5 | 6.5 | 1730 | 1551.5 | 10.3 |
| 1.6 | 3.9 | 1796 | 1698.8 | 5.4 |
| 1.7 | 4.2 | 1825 | 1685.4 | 7.7 |
| 2.0 | 4.7 | 1817 | 1658.9 | 8.7 |
| 2.1 | 5.1 | 1753 | 1637.8 | 6.6 |
| 2.1 | 5.2 | 1772 | 1632.9 | 7.9 |
| 2.5 | 6.3 | 1732 | 1562.5 | 9.8 |
| 2.5 | 6.8 | 1713 | 1535.1 | 10.4 |

Standard error obtained is 0.079

**Table 5: Comparison of analytical and experimental fracture strength of M250 grade maraging steel parent metal SCT specimens [7]**
**($W$=15mm, $t$= 7.5mm, $\sigma_{ult}$ =1720MPa, $K_F$ =235.7 MPa, $m$=0.6, $p$=20.4)**

| Crack Dimensions (mm) | | Fracture strength $\sigma_f(MPa)$ | | |
|---|---|---|---|---|
| $a$ | $2c$ | Test | Analysis | Relative Error (%) |
| 1.3 | 2.7 | 1735 | 1627.0 | 6.2 |
| 1.5 | 2.7 | 1713 | 1620.0 | 5.4 |
| 1.0 | 2.8 | 1700 | 1625.4 | 4.4 |
| 1.1 | 2.8 | 1752 | 1624.5 | 7.3 |
| 1.7 | 3.8 | 1711 | 1592.9 | 6.9 |

| Crack Dimensions (mm) | | Fracture strength $\sigma_f(MPa)$ | | |
|---|---|---|---|---|
| $a$ | $2c$ | Test | Analysis | Relative Error (%) |
| 1.5 | 3.9 | 1706 | 1591.5 | 6.7 |
| 1.4 | 3.9 | 1700 | 1592.9 | 6.3 |
| 1.5 | 4.0 | 1736 | 1588.7 | 8.5 |
| 1.6 | 4.8 | 1711 | 1564.6 | 8.6 |
| 2.2 | 5.0 | 1666 | 1546.8 | 7.2 |
| 2.0 | 5.0 | 1682 | 1549.8 | 7.9 |
| 2.0 | 5.3 | 1621 | 1539.3 | 5.0 |
| 2.2 | 5.4 | 1654 | 1531.4 | 7.4 |
| 1.9 | 5.7 | 1616 | 1528.8 | 5.4 |
| 2.3 | 6.0 | 1581 | 1506.5 | 4.7 |
| 2.7 | 6.2 | 1590 | 1485.6 | 6.6 |
| 2.2 | 6.6 | 1590 | 1485.5 | 6.6 |
| 2.2 | 6.8 | 1553 | 1478.0 | 4.8 |

Standard error obtained is 0.066

## 4. Failure Assessment Diagram (FAD)

Failure assessment diagram is widely employed to ensure the safety of defected engineering or structural components. FAD helps to address the acceptable and unacceptable range of a material. FAD for Table 2 through 5 are given below.

For both figures $K_{\max}$ is plotted along horizontal axis and $\sigma_f/\sigma_{ult}$ ratio along vertical axis. In Figurer-2, Dark line represents curve for M300 Marging steel specimen data given in Table-2, whereas dotted curve corresponds to the specimen data of M300 given in Table-3. Similarly, in Figure-3, dark line represents curve for data given in Table-4 and the dotted line refers to that of the data provided in Table-5. From the figures plotted, one can easily identify the safe region for process. As the fracture behavior of the particular material depends on the mechanical properties, the nature of crack observed and the type of process that the material undergoes. FAD clearly dictates the safe region for design process. The area within the curve is the acceptable region and the area outside the curve is the unacceptable region for the concerned material.

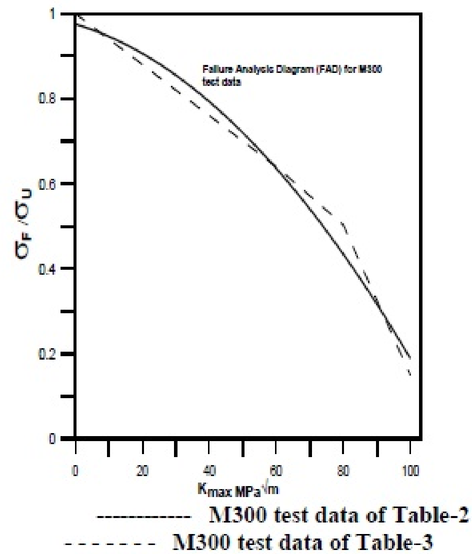


**Fig 2: Failure Analysis Diagram for M300 test data.**

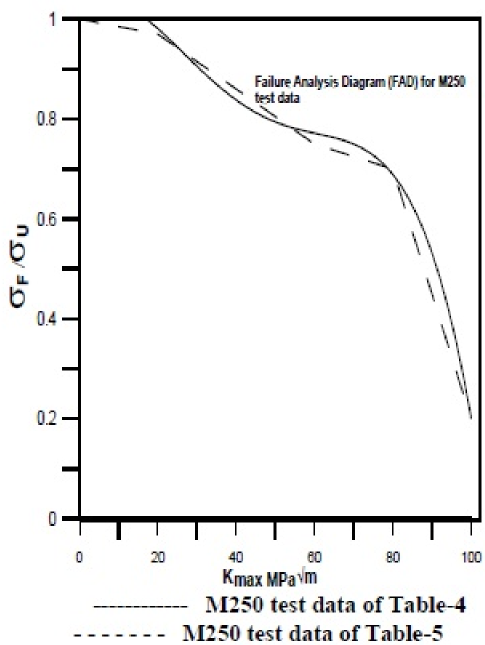


**Fig 3: Failure Analysis Diagram for M250 test data.**

## 5. Conclusion

Fracture strength of M250 and M300 grade maraging steel parent surface cracked specimens has been evaluated analytically and compared with the test data. From the procedure developed, relative error between the analytical and the tested data computed and presented in the Tables. Failure assessment diagrams for both the M250 and M300 grade maraging steel specimens generated and presented. The procedure demonstrated would bring the designer and the fabrication engineers in understanding the design life of the component.

**Acknowledgement**

One of the authors Smt. Sreedevi Lekshmi expresses her gratitude for the opportunity provided to pursue her M. Tech. project in VSSC. The authors also wish to thank Shri. Sirajudeen Ahamed, Group Director, Structural Design and Engineering Group and Dr. Unnikrishnan Nair S, Deputy Director, Structural Engineering Entity (STR) of Vikram Sarabhai Space Centre (VSSC), for their encouragements; Dr. K. Sivan, Director, VSSC for giving permission to publish this paper. Thanks are due to VSSC Editorial Board for making necessary arrangements to review the paper for publication.

## References

[1] Sundaresan S., Manirajan M. and Nageswara Rao B., On the fracture toughness evaluation in weldments of a maraging steel rocket motorcase, Materials and design, 31 (2010), 4921-4926.

[2] ASTM E399-06, Stantard Test Method for Linear Elastic Plane-Strain-Fracture Toughness KIC of Metallic Materials, Annual Book of ASTM Stantards-03.01, (2008).

[3] Singaravelu J., Sundaresan S., Nageswara Rao B., Application of fracture mechanics to specify the proof load factor for clamp band systems of launch vehicles, Journal of Material Engineering and Performance, 22(Issue 4) (2010), 926-935.

[4] Navmen Jr. J. C., Fracture analysis of surface and through cracks in cylindrical pressure vessels, NASA-TND-8325 (1976).

[5] Nageswara Rao B. and Acharya A. R., Structural Integrity Assessment on M250 grade maraging steel pressure vessels via FM approach, Journal of the Aeronautical Society of India, 45 (1993), 308-322.

[6] Perl M. and Levinsohn J. A., Measurement of the actual fracture toughness of a maraging -300 pressurised cylinder using the vessel as the test specimen. Engineering Fracture Mechanics, 34 (1989), 525-530.

[7] Diwakar V., Arumugam S., Lakshmanam T. S. and Sarkar B. K., Residual strength of maraging steelh, Journal of Material Science, 24 (1989), 1268-1272.